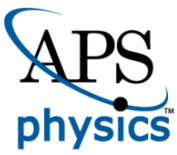

Mitigation of stimulated Raman scattering in the kinetic regime by external magnetic fields

B. J. Winjum, F. S. Tsung, and W. B. Mori

Phys. Rev. E **98**, 043208 — Published 29 October 2018

DOI: 10.1103/PhysRevE.98.043208

Mitigation of stimulated Raman scattering in the kinetic regime by external magnetic fields

B. J. Winjum,[1,2] F. S. Tsung,[2,3] and W. B. Mori[1,2,3,4]

[1]*Institute for Digital Research and Education, University of California Los Angeles, Los Angeles, CA 90095*
[2]*Particle-in-Cell and Kinetic Simulation Software Center, University of California Los Angeles, Los Angeles, CA 90095*
[3]*Department of Physics & Astronomy, University of California Los Angeles, Los Angeles, CA 90095*
[4]*Department of Electrical Engineering, University of California Los Angeles, Los Angeles, CA 90095*

(Dated: October 2, 2018)

We show via particle-in-cell simulations that small normalized magnetic fields ($\omega_c/\omega_p \ll 1$) can significantly modify the evolution of backward stimulated Raman scattering (SRS) in the kinetic regime due to the enhanced dissipation of nonlinear electron plasma waves propagating perpendicular to magnetic fields. A magnetic field applied perpendicularly to the electron plasma wave (and driving light wave) increases the SRS threshold for kinetic inflation and decreases the amount of reflectivity when SRS is driven significantly above threshold. Analysis indicates this arises because trapped electrons are accelerated as they surf across the wave, leading to the continual dissipation of the electron plasma waves over a wider range of wave amplitudes. The reduction in SRS reflectivity is most significant for a purely perpendicular field, though reduction also occurs for other angles; a parallel field can slightly increase single-speckle SRS but decreases multi-speckle SRS. These simulations demonstrate the significance of magnetic field contributions to nonlinear electron plasma wave damping with respect to nonlinear parametric decay instabilities; the simulation parameters are directly relevant for SRS in inertial confinement fusion devices and indicate that approximately 30 Tesla magnetic fields might significantly reduce SRS backscatter.

The nonlinear damping of an electron plasma wave (EPW) propagating perpendicularly to a magnetic field is a topic of fundamental interest, albeit one which has not been very widely studied. Sagdeev and Shapiro [1] and Dawson *et al.* [2] realized over 35 years ago that EPWs in such a scenario can be profoundly affected by even weak fields due to the fact that trapped electrons (those moving near the EPW phase velocity v_ϕ) in an average sense all get accelerated perpendicularly across the wave front, continually extracting energy from it. The "surfatron" electron acceleration mechanism has been studied with respect to particle accelerators [3], astrophysical particle acceleration in shocks and upper-hybrid waves [4, 5], and phasespace hole dynamics [6], but the concomitant wave damping has not been appreciated in any significant context and has been studied by only a few authors [7, 8].

The damping of kinetic EPWs in even weak magnetic fields could have potentially dramatic consequences for instabilities whose evolution is sensitive to the nonlinear damping of large-amplitude EPWs. For example, in the stimulated Raman scattering (SRS) of a laser beam in inertial confinement fusion (ICF) [9], where the laser light decays into scattered light and electron plasma waves, the EPWs evolve in a regime in which resonant wave-particle interactions reduce the EPWs' damping rate (leading to kinetic inflation [10, 11]), alter its frequency, bend its wavefronts, change its envelope shape, and couple it with other plasma modes (e.g., [12–16]). Interestingly, magnetic fields are increasingly being studied in the context of ICF, including for MagLIF [17, 18]; for imposing external magnetic fields to affect implosion dynamics, fusion reactivity, and hot electron propagation [19–21]; and potentially for applying external magnetic fields to alter SRS dynamics by increasing the electron temperature [22] or limiting electron motion transverse to laser speckles [14]. However, the consequence of magnetic fields to the kinetic evolution of EPWs, and thereby its consequence for the detrimental SRS instability, have not been studied.

Here we show for the first time that applying an external B-field perpendicularly to EPWs in SRS can quench the instability. This limiting effect on SRS is due to the damping effect on nonlinear EPWs propagating across an external B-field. The amplitude of magnetic fields required to significantly reduce SRS are dependent on the parameter regime, though for the cases considered here are on the order of 10's of Tesla. It is outside the scope of this article to examine how such fields might be realized experimentally within ICF-relevant plasmas, but our parameters are within the ranges recently studied by other authors in experiments and/or rad-hydro modeling [19–27]. We note that even though the plasma β is very large, rad-hydro modeling has shown that the applied magnetic fields persist [21]. In addition, fields of the strength considered here can be self-generated in ICF-relevant plasmas [28, 29].

We consider parameters where $\bar{\omega}_c \equiv \omega_c/\omega_p \ll 1$, where ω_c and ω_p are the electron cyclotron and plasma frequencies, respectively ($\bar{\omega}_c = 3.3 \times 10^6 B_{Tesla}/(n_{cm^{-3}})^{1/2}$). In this regime, the EPW's real frequency is essentially its unmagnetized value (and Faraday rotation of the light waves is negligible for magnetic fields aligned with the laser). Furthermore, we study parameters for which SRS is in the strongly damped regime but for which the EPWs in SRS evolve toward undamped modes in an unmagne-

tized plasma due to resonant wave-particle interactions, i.e., for conditions in which the EPW Landau damping rate γ_{LD} is comparable to or greater than the temporal SRS growth rate [30] and in which γ_{LD} is smaller than the trapped particle bounce frequency $\omega_B \equiv \sqrt{eE_0k/m}$, where E_0 and k are the EPW's amplitude and wavenumber. We note that $\omega_B/\omega_p \equiv \sqrt{\frac{eE_0k}{m\omega_p^2}} \cong \sqrt{\epsilon}$, where ϵ is E_0 normalized to the cold wavebreaking value [31].

As shown in Dawson *et al.* [2], for an EPW of the form $\vec{E} = E_0 \sin(kx - \omega t)\hat{x}$ propagating perpendicular to a field $\vec{B} = B_0\hat{z}$, the equations of motion for an electron in the wave frame are: $\ddot{v}'_x + \omega'^2_B v'_x = -\omega_c^2 v_\phi$ and $\dot{v}_y = \omega_c v_x$, where $\omega'_B = \sqrt{\omega_c^2 + \omega_B^2\cos(kx)}$ and primed quantities ($'$) are defined in the wave frame. A resonant electron will execute bounce motion at roughly the modified frequency ω'_B while it is accelerated (deflected) transversely across the wave front. As this occurs, the resulting v_yB_0 force causes the electron to slowly drift backwards in the wave frame. In 1D, and if the electron starts near rest at the bottom of the wave's potential ($-e\phi$), i.e., at a zero of the electric field where its slope is positive, the particle will continue to execute this modified bounce motion until the $E_x + \frac{v_y}{c}B_0$ force vanishes, at which time the electron will be detrapped with $v_y = c\frac{E_x}{B_0}$. However, if the electron starts at different locations in the potential well, or if it begins with a large v_x as might occur if the trapping width is large, then it can exit with a value of v_y more than an order of magnitude less than $c\frac{E_x}{B_0}$. Furthermore, for SRS in high energy density plasmas, there is a spectrum of plasma waves, the plasma wave amplitudes and phases are continually changing, and relativistic effects can be important. For ICF parameters, $\frac{E_x}{B_0} \gg 1$ but relativistic corrections and additional detrapping processes can be present. Even in 1D, the de-trapping is more complicated because the wave amplitude and phase velocity are evolving and the wave is not monochromatic. In 2D and 3D, an electron moving across the wave front of a finite-width wave can additionally be detrapped because it leaves the wave. Nevertheless, in all cases, by accelerating across the wave front all trapped electrons will now only extract energy from the wave.

To study how this nonlinear damping affects SRS, we carry out one- and two-dimensional (1D and 2D) simulations using the electromagnetic particle-in-cell (PIC) code OSIRIS 4.0 [32]. The electrons have a temperature $T_e = 3$ keV and slight linear density gradient $n_e = 0.128 - 0.132n_{cr}$ ($k\lambda_D \approx 0.30$ for backward SRS); ions are fixed to focus solely on SRS interactions. We simulate an f/8 speckled laser beam of wavelength $\lambda_0 = 0.351\mu$m, and in the single-speckle case we emulate a single f/8 speckle with a Gaussian laser beam with focal width $f\lambda_0 = 2.8\mu$m (intensity full-width half-max) launched from an antenna at the boundary. The quoted laser intensities are at the focus and range over $6 \times 10^{14} - 5 \times 10^{15}$ W/cm^2 (where the normalized field of the laser $eE/mc\omega_0 \equiv eA/mc^2 = 8.5 \times 10^{-10}\sqrt{I(W/cm^2)}\lambda_0(\mu m) = 0.00735{-}0.0212$). The laser propagates along $\hat{x}$ and is polarized in the 2D plane in $\hat{y}$; B_{ext} is applied in $\hat{z}$, though similar results have been seen by applying B_{ext} in the $\hat{y}$ direction. The 2D laser profile is only finite-width in $\hat{y}$, so resonant electrons can only be kicked out of the speckle by traveling in the $\hat{y}$ direction. We used 512 (256) particles per cell in 1D (2D) simulations with cubic interpolation, a grid with 10740 x 1194 cells, and a simulation box of size 120 x 20 μm^2. The length corresponds to the central portion of an $f/8$ speckle of length $5f^2\lambda_0 = 120\mu$m. We simulate approximately 6 ps in time. The multi-speckle simulations have a width of 42 μm (approximately 15 speckle widths) with absorbing boundaries for the fields and thermal-bath boundaries for the particles in $\hat{x}$ but periodic boundaries in $\hat{y}$. For the single-speckle simulations, we use absorbing and thermal boundaries in both $\hat{x}$ and $\hat{y}$ in order to prevent the speckle from interacting with energetic particles and scattered light that would otherwise re-circulate in the transverse direction. This has the further consequence that exiting particles do not retain their gyro motion when crossing the boundary. However, single speckle simulations with periodic boundaries show similar features. Furthermore, the single speckle simulations here are illustrative of the relevant physics and the multi-speckle simulations retain all proper cyclotron motion of the particles.

B_{ext} ranges up to 50 T. For $B_{ext} = 15$ T (60 T), the normalized cyclotron frequency $\bar{\omega}_c = 0.001$ (0.005). In a plasma with $T_e = 3$ keV and $T_i = 1$ keV, the Larmor radius for a thermal electron is $r_e = 8\mu$m (2 μm) and for a thermal proton is $r_i = 20$ mm (0.5 mm). The electron (ion) cyclotron period is on the order of a picosecond (nanosecond). For the single-speckle SRS shown here, the speckle width is on the same order as r_e (several microns) and the time for an e-folding of SRS is on the order of the gyro period (picoseconds). The ions will execute a gyro period on a time scale much longer than the timescales of interest for the kinetic bursts of SRS. We have performed several mobile ion simulations and found the conclusions drawn here to be unchanged.

The ability of an external magnetic field to decrease SRS activity is evident in 1D simulations ($1\frac{2}{2}$, i.e., one spatial but three velocity components). Figure 1a shows the spatio-temporal behavior of EPWs for 1D simulations with $T_e = 3$keV, $I_0 = 3 \times 10^{15}$W/cm^2, and $B_{ext} = 0$ and 30T. For $B_{ext} = 0$, strong SRS is seen with the growth and convection of EPWs over most of the simulated domain and time; SRS EPW amplitudes in this regime can be on the order of $\epsilon \approx 0.1$. With $B_{ext} = 30$T, on the other hand, the EPW behavior is much more limited in time for each burst of SRS, the EPW peak amplitudes are slightly lower, and the total time-averaged reflectivity level is decreased. To demonstrate the increased damping of EPWs in the presence of B_{ext}, we did two exactly similar simulations with the exception that the driving laser was turned off after $\omega_0 t = 4300$. Figure 1b shows that, for $B_{ext} = 0$, the SRS-driven EPWs continue to propagate relatively undamped after the laser is turned off, whereas

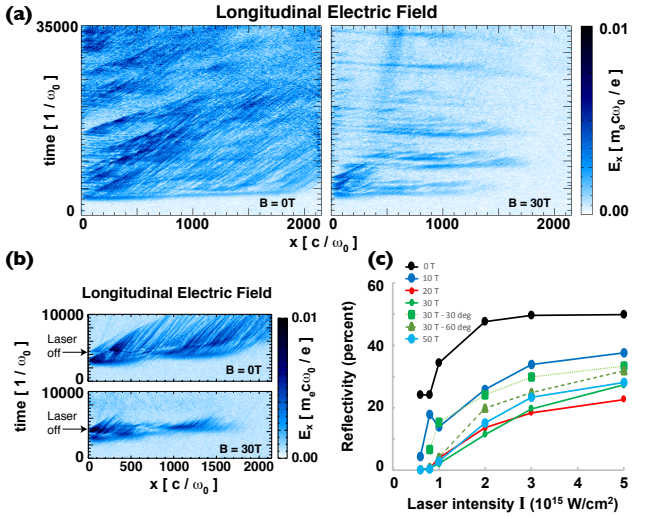

FIG. 1: (a) Time vs space plots of EPW activity in a continuously driven system with $B_{ext} = 0$ (left) and 30T (right); (b) similar plots when turning the driving laser off at $\omega_0 t = 4300$; and (c) time-averaged reflectivity vs laser intensity for several magnetic field amplitudes and orientations in continuously driven simulations.

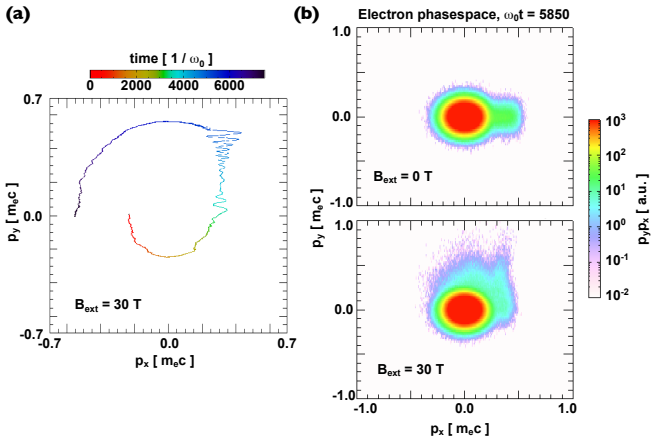

FIG. 2: (a) One particle track plotted in $p_y p_x$ space over $\omega_0 t = 0 - 7500$. (b) Domain-averaged $p_y p_x$ space near the time of initial SRS saturation for $B_{ext} = 0$ (top) and 30T (bottom).

for $B_{ext} = 30$T they are very quickly damped after the laser turns off, supporting the argument that one must account for the additional damping of nonlinear EPWs in magnetic fields in order to accurately determine the dynamics of SRS in these scenarios.

Time-averaged reflectivities across a range of laser intensities and B-field amplitudes are shown in Figure 1c. At the kinetic threshold where SRS just begins to reflect light, B_{ext} decreases the reflectivity to 0. For larger intensities, the reflectivity can be decreased by at least 50%. For constant laser intensity, the reflectivity decreases for increasing B_{ext}, though the decrease appears to asymptote and progressively larger B_{ext} are not always able to decrease these 1D reflectivities to 0. We also show two curves for B_{ext} oriented in the x-z plane at angles of 30 and 60 degrees relative to $\hat{x}$. The reflectivity decreases progressively more as the orientation increases from 30 to 60 to 90 degrees, demonstrating that even if B_{ext} is not purely perpendicular, the component along the perpendicular direction can still have a similar effect on SRS. The effect of geometry is an area for future work.

To investigate the mechanism behind this decrease in SRS, we show illustrative plots of electron phasespace in Figure 2. One representative trapped particle orbit is shown in Figure 2a in $p_x p_y$ phasespace, where unperturbed electrons gyrate counter-clockwise in the B-field. The shown particle approaches the EPW phase velocity ($p_x/m_e c \approx 0.3$) and oscillates about this value as it bounces in the wave. While it is trapped, the electron is accelerated across the EPW wavefront in p_y. Eventually the particle detraps, at which point it continues executing cyclotron motion with a larger energy. The particle gains enough momentum in $\hat{y}$ that its correct velocity in v_x must be considered relativistically, illustrating that for ICF parameters relativistic corrections need to be included. In addition, it is accelerated to an energy of approximately 75 keV; if such particles are not confined by the B-field and escape towards the fuel target, they could be a pre-heat threat. The acceleration of many electrons in such a manner is evidenced in Figure 2b. For the case with $B_{ext} = 0$, particle acceleration by SRS-generated EPWs is predominantly in the p_x direction and up to a maximum of $p_x/m_e c \approx 0.5$. For $B_{ext} = 30$T on the other hand, trapped electrons with $p_x/m_e c \approx 0.3$ are accelerated in p_y (and accelerated to momenta > 0.5); once detrapped, these energetic particles gyrate about the field, as evidenced for example by the range of energetic particles with $p_x/m_e c \ll 0.3$ and $p_y/m_e c > 0.3$. This cross field acceleration mechanism is sufficient to disrupt the nonlinear damping of EPWs during and after SRS saturation and to severely impact the time-averaged behavior of the instability.

We next look at simulations of SRS in single laser speckles with $I_0 = 3 \times 10^{15}$ W/cm^2. Figure 3a shows the time-averaged reflectivity as a function of B-field strength for orientations both parallel and perpendicular to the laser k_0 ($\hat{x}$ and $\hat{z}$ directions, respectively). As the B-field increases in magnitude, the reflectivity decreases significantly for the perpendicular case while increasing slightly for the parallel case. For these single speckle simulations, the waves have a finite width and the B-field can now not only accelerate trapped particles across the EPW wavefronts but also deflect them out of an unstable region in physical space. This results in a novel kinetic evolution of finite-width EPWs, as evidenced in Figure 3b, where snapshots of nonlinear EPWs for $B_{ext} = 0$ and 50 T are shown. For $B_{ext} = 0$, the wavefronts are bowed symmetrically about the central axis due to the nonlinear frequency shift on either side of the EPW and the wave is broken up due to the trapped particle modulational

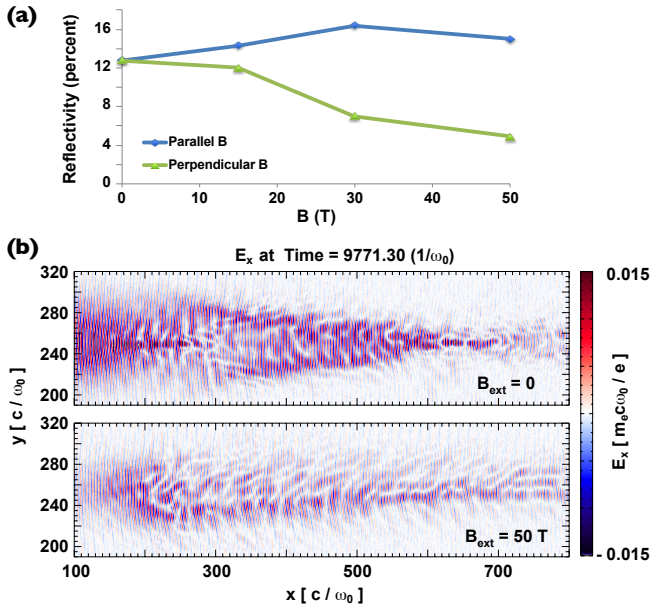

FIG. 3: (a) Time-averaged SRS reflectivity as a function of B-field amplitudes. (b) Snapshots in time of 2D EPWs during SRS.

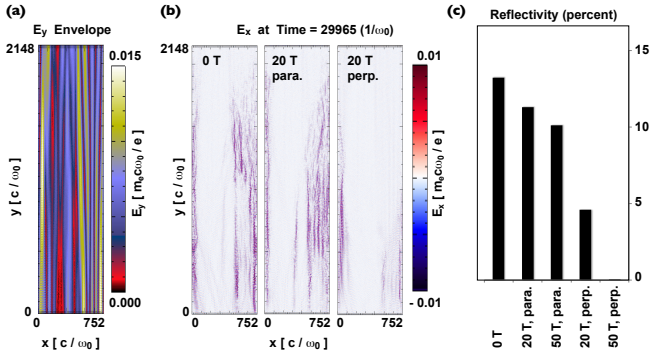

FIG. 4: (a) Representative snapshot of the incident laser envelope early in time. (b) Snapshots in time of EPW activity for $B_{ext} = 0$, 20T parallel, and 20T perpendicular; (c) Time-averaged reflectivities for different B_{ext}.

instability. When there is a perpendicular B_{ext}, on the other hand, trapped particles traveling in $\hat{x}$ are accelerated in the $\hat{y}$-direction by B_{ext}, resulting in nonlinear damping that is different on the top-half of the EPW than on the bottom-half. The wavefronts are bowed on the bottom half of the spatial domain but, in the top half of the domain, the EPW packet is much lower in amplitude and more disrupted in space.

Although not shown, for B_{ext} parallel to k_0, there is negligible visible difference in EPW behavior outside of what looks like statistical variability, though the EPW activity grows over a longer part of the spatial domain than in the case with $B_{ext} = 0$. With B_{ext} aligned with the wave vectors of the incident laser and the SRS EPW, the trapped particles gyrate in $\hat{y}$ and $\hat{z}$ and, in the absence of relativistic mass corrections, they still execute normal bounce oscillations in the parallel direction. Since they are more strongly confined to the speckle region, there is less trapped-particle side-loss and the SRS ends up being more 1D-like. This can give more SRS and higher reflectivity, though here the gyroradius of an electron moving at the phase velocity is larger than the speckle width and the increase in SRS is relatively slight.

Finally, we simulated SRS in a multi-speckled laser beam with $I_{ave} = 8 \times 10^{14}$ W/cm^2. The incident laser profile is shown in Figure 4a. SRS in multi-speckled laser beams can grow as a collective phenomenon due to the spray of waves and particles out of an SRS-unstable region [14, 33, 34]. Consequently, the effect of B_{ext} on multi-speckled SRS depends not just on its influence on single bursts but also on its effect on how waves and particles generated in one burst can travel into other regions that have not yet become unstable. While we have shown that B_{ext} aligned with k_0 can act to enhance SRS activity, it also limits the transverse motion of trapped particles, and this in turn limits collective multi-speckle SRS (as was hypothesized by Yin *et al.* [14]). Figure 4b shows it is difficult to distinguish the EPW activity generated by SRS bursts in a case with no B field versus that with a 20 T field aligned with k_0.

For B_{ext} perpendicular to k_0, on the other hand, the decrease in plasma wave activity (fourth plot from left) and reflectivity (right plot) is much more pronounced. This appears to be due to several reasons. First, the crossed B-field can prevent an undamped EPW from forming, thereby greatly reducing the number of speckles that are above the laser intensity for kinetically inflated activity. Second, SRS activity in above-threshold speckles is reduced by EPW damping in the crossed B-field. Third, the impact of SRS from above-threshold speckles on neighboring speckles is reduced, both because their production of scattered light waves and trapped particles is reduced and because it is more difficult to trigger SRS in neighboring below-threshold speckles since they are "further" from threshold. Finally, the spatial range of trapped particles is confined more closely to existing regions of instability by the cyclotron motion due to B_{ext}.

While we have shown that magnetic fields may dramatically affect the evolution of SRS, changing the threshold of SRS in a density gradient may make SRS grow predominantly at higher densities, or lower $k\lambda_D$, and SRS in higher density regions may have higher saturation levels. Furthermore, B-fields could potentially increase (rather than decrease) SRS by interfering with the nonlinear frequency shift and limiting the effect of detuning which can saturate SRS. Bandwidth (ISI [35] and SSD [36]) and/or STUD pulses [37–39] combined with magnetic fields may work well, as the EPW may dissipate more strongly during times when the laser is "off" at some spatial location. Finally, other instabilities may be affected by B fields, such as the two plasmon and high frequency hybrid instability. The kinetic evolution of nonlinear plasma waves in weakly magnetized plasmas is therefore a ripe area for

research.

This work was supported by DOE under Grant No. DE-NA0002953 and the NSF under Grant No. ACI-1339893. Simulations were performed on the UCLA Dawson2 (NSF PHY 0960344) and UCLA Hoffman2 Clusters, NSF's BlueWaters, and ALCF's Mira.

[1] R. Z. Sagdeev and V. D. Shapiro, JETP Lett. **17**, 279 (1973).
[2] J. M. Dawson, V. K. Decyk, Robert W. Huff, I. Jechart, T. Katsouleas, J. N. Leboeuf, B. Lembege, R. M. Martinez, Y. Ohsawa, and S. T. Ratliff, Phys. Rev. Lett. **50**, 1455 (1983).
[3] T. Katsouleas and J. M. Dawson, Phys. Rev. Lett. **51**, 392 (1983).
[4] V. D. Shapiro and D. Ucer, Planetary and Space Science **51**, 665 (2003).
[5] M. E. Dieckmann, B. Eliasson, and P. K. Shukla, Astrophysical Journal **617**, 1361 (2004).
[6] B. Eliasson, M. E. Dieckmann, and P. K. Shukla, New Journal of Physics **7**, 136 (2005).
[7] B. E. Gribov, R. Z. Sagdeev, V. D. Shapiro, and V. I. Shevchenko, Pis'ma Zh. Eksp. Teor. Fiz. **42**, 54 (1985) [JETP Lett. 42, 63 (1985)].
[8] V. L. Krasovsky, Fizika Plazmy **33**, 914 (2007) [Plasma Physics Reports **33**, 839 (2007)].
[9] R. Betti and O. A. Hurricane, Nature Physics **12**, 435 (2016).
[10] H. X. Vu, D. F. DuBois, and B. Bezzerides, Phys. Plasmas **14**, 012702 (2007).
[11] I. N. Ellis, D. J. Strozzi, B. J. Winjum, F. S. Tsung, T. Grismayer, W. B. Mori, J. E. Fahlen, and E. A. Williams, Phys. Plasmas **19**, 112704 (2012).
[12] L. Yin, B. J. Albright, K. J. Bowers, W. Daughton, and H. A. Rose, Phys. Rev. Lett. **99**, 265004 (2007).
[13] L. Yin, B. J. Albright, K. J. Bowers, W. Daughton, and H. A. Rose, Phys. Plasmas **15**, 013109 (2008).
[14] L. Yin, B. J. Albright, H. A. Rose, D. S. Montgomery, J. L. Kline, R. K. Kirkwood, P. Michel, K. J. Bowers, and B. Bergen, Phys. Plasmas **20**, 012702 (2013).
[15] B. J. Winjum, "Particle-in-cell simulations of stimulated Raman scattering for parameters relevant to inertial fusion energy," Ph.D. dissertation, University of California, Los Angeles (2010).
[16] B. J. Winjum, J. E. Fahlen, F. S. Tsung, and W. B. Mori, Phys. Rev. E **81**, 045401(R) (2010).
[17] S. A. Slutz and R. A. Vesey, Phys. Rev. Lett. **108**, 025003 (2012).
[18] A. B. Sefkow, S. A. Slutz, J. M. Koning, M. M. Marinak, K. J. Peterson, D. B. Sinars, and R. A. Vesey, Phys. Plasmas **21**, 072711 (2014).
[19] L. J. Perkins, B. G. Logan, G. B. Zimmerman, and C. J. Werner, Phys. Plasmas **20**, 072708 (2013).
[20] D. J. Strozzi, L. J. Perkins, M. A. Rhodes, B. G. Logan, D. D. Ho, G. B. Zimmerman, S. A. Hawkins, D. T. Blackfield, Anomalous Absorption Conference (2015).
[21] D. J. Strozzi, L. J. Perkins, M. M. Marinak, D. J. Larson, J. M. Koning, and B. G. Logan, J. Plasma Phys. **81**, 475810603 (2015).
[22] D. S. Montgomery, B. J. Albright, D. H. Barnak, P. Y. Chang, J. R. Davies, G. Fiksel, D. H. Froula, J. L. Kline, M. J. MacDonald, A. B. Sefkow, L. Yin, and R. Betti, Phys. Plasmas **22**, 010703 (2015).
[23] H. Daido, F. Miki, K. Mima, M. Fujita, K. Sawai, H. Fujita, Y. Kitagawa, S. Nakai, and C. Yamanaka, Phys. Rev. Lett. **56**, 846 (1986).
[24] D. H. Froula, J. S. Ross, B. B. Pollock, P. Davis, A. N. James, L. Divol, M. J. Edwards, A. A. Offenberger, D. Price, R. P. J. Town, G. R. Tynan, and S. H. Glenzer, Phys. Rev. Lett. **98**, 135001 (2007).
[25] O.V. Gotchev, P.Y. Chang, J. P. Knauer, D. D. Meyerhofer, O. Polomarov, J. Frenje, C. K. Li, M. J.-E. Manuel, R. D. Petrasso, J. R. Rygg, F. H. Séguin, and R. Betti, Phys. Rev. Lett. **103**, 215004 (2009).
[26] G. Fiksel, W. Fox, A. Bhattacharjee, D. H. Barnak, P.-Y. Chang, K. Germaschewski, S. X. Hu, and P. M. Nilson, Phys. Rev. Lett. **113**, 105003 (2014).
[27] C. Goyon, B. B. Pollock, D. P. Turnbull, A. Hazi, L. Divol, W. A. Farmer, D. Haberberger, J. Javedani, A. J. Johnson, A. Kemp, M. C. Levy, B. Grant Logan, D. A. Mariscal, O. L. Landen, S. Patankar, J. S. Ross, A. M. Rubenchik, G. F. Swadling, G. J. Williams, S. Fujioka, K. F. F. Law, and J. D. Moody, Phys. Rev. E **95**, 033208 (2017).
[28] W. A. Farmer, J. M. Koning, D. J. Strozzi, D. E. Hinkel, L. F. Berzak Hopkins, O. S. Jones, and M. D. Rosen, Phys. Plasmas **24**, 052703 (2017).
[29] A. S. Joglekar, C. P. Ridgers, R. J. Kingham, and A. G. R. Thomas, Phys. Rev. E **93**, 043206 (2016).
[30] D. W. Forslund, J. M. Kindel, and E. L. Lindman, Phys. Fluids **18**, 1002 (1975).
[31] J. M. Dawson, Phys. Rev. **113**, 383 (1959).
[32] R. G. Hemker. Ph.D. thesis, University of California, Los Angeles, 2000; R.A. Fonseca *et al.*, Lecture Notes in Computer Science **2331**, 342 (2002); R.A. Fonseca *et al.*, Plasma Physics and Controlled Fusion **50**, 124034 (2008).
[33] L. Yin, B. J. Albright, H. A. Rose, K. J. Bowers, B. Bergen, R. K. Kirkwood, D. E. Hinkel, A. B. Langdon, P. Michel, D. S. Montgomery, and J. L. Kline, Phys. Plasmas **19**, 056304 (2012).
[34] B. J. Winjum, A. Tableman, F. S. Tsung, and W. B. Mori, to be submitted (2018).
[35] S. P. Obenschain, C. J. Pawley, A. N. Mostovych, J. A. Stamper, J. H. Gardner, A. J. Schmitt, and S. E. Bodner. Phys. Rev. Lett. **62**, 768 (1989).
[36] B. J. Macgowan, B. B. Afeyan, C. A. Back, R. L. Berger, et al. Phys. Plasmas **3**, 2029 (1996).
[37] B. Afeyan and S. Hüller, Eur. Phys. J. Web Conf. **59**, 05009 (2013).
[38] S. Hüller and B. Afeyan, Eur. Phys. J. Web Conf. **59**, 05010 (2013).
[39] B. J. Albright, L. Yin, and B. Afeyan, Phys. Rev. Lett. **113**, 045002 (2014).